



This is a repository copy of *Impact ionization in InAs electron avalanche photodiodes*.

White Rose Research Online URL for this paper:
<http://eprints.whiterose.ac.uk/42655/>

Article:

Marshall, A.R.J., David, J.P.R. and Tan, C.H. (2010) Impact ionization in InAs electron avalanche photodiodes. *IEEE Transactions on Electron Devices*, 57 (10). pp. 2631-2638. ISSN 0018-9383

<https://doi.org/10.1109/TED.2010.2058330>

Reuse

Unless indicated otherwise, fulltext items are protected by copyright with all rights reserved. The copyright exception in section 29 of the Copyright, Designs and Patents Act 1988 allows the making of a single copy solely for the purpose of non-commercial research or private study within the limits of fair dealing. The publisher or other rights-holder may allow further reproduction and re-use of this version - refer to the White Rose Research Online record for this item. Where records identify the publisher as the copyright holder, users can verify any specific terms of use on the publisher's website.

Takedown

If you consider content in White Rose Research Online to be in breach of UK law, please notify us by emailing eprints@whiterose.ac.uk including the URL of the record and the reason for the withdrawal request.



eprints@whiterose.ac.uk
<https://eprints.whiterose.ac.uk/>

Impact Ionization in InAs Electron Avalanche Photodiodes

Andrew R. J. Marshall, John P. R. David, *Senior Member, IEEE*, and Chee Hing Tan, *Member, IEEE*

Abstract—A systematic study of impact ionization, avalanche multiplication, and excess noise in InAs diodes has been carried out, confirming that avalanche multiplication is dominated by the impact ionization of electrons. This results in highly desirable “electron avalanche photodiode” characteristics previously only demonstrated in HgCdTe diodes, which are discussed in detail. The suppression of excess noise by nonlocal effects, to levels below the local model minimum of $F = 2$, is explained. An electron ionization coefficient is calculated and shown to be capable of modeling the electron impact ionization, which differs characteristically from that in wider bandgap III–V materials.

Index Terms—Avalanche photodiode (APD), electron avalanche photodiode (e-APD), impact ionization, InAs, ionization coefficient.

I. INTRODUCTION

THE PROCESS of impact ionization and its exploitation in avalanche photodiodes (APDs) has been thoroughly investigated in most established semiconductor materials with bandgap energies greater than 1 eV. In contrast, there have been few investigations in semiconductor materials with bandgaps below that of $\text{In}_{0.53}\text{Ga}_{0.47}\text{As}$ and few reports of APDs detecting at wavelengths beyond its 1.7- μm cutoff. There are, however, emerging applications in the short-wave and midwave infrared, which could exploit APDs to improve overall system sensitivity. These are typically low photon flux or high bandwidth applications such as active imaging, hyperspectral imaging, atmospheric gas monitoring, and free space communications. Hence, there is increasing interest in the investigation of impact ionization in narrower bandgap materials for potential use in APDs. Furthermore, since the excess noise generated by any APD is dependent on the material properties of its gain medium, there is a long standing cross-application interest in identifying materials with favorable properties [1].

In all APDs, avalanche gain is accompanied by an increase in noise power, characterized by the gain-dependent excess noise factor F . In order to minimize F and maximize the extent to which an APD’s gain can be exploited before its noise begins to dominate the system noise, the electron ionization coefficient α and the hole ionization coefficient β should be as disparate as

possible. Ideally, either α or β should be equal to zero, such that the ionization coefficient ratio $k = \alpha/\beta$ or $k = \beta/\alpha$ also becomes zero. In this ideal case, F asymptotically approaches 2 as gain increases, under the local model of impact ionization [2]. Furthermore, an APD’s bandwidth is also reduced with increasing values of k [3]. Unfortunately, in established wider bandgap III–V materials, it has been found that both carrier types undergo significant impact ionization resulting in k values between approximately 1 and 0.1 [1], [4]. It is for this reason that III–V APDs suffer from higher levels of noise than silicon APDs.

Amongst narrower bandgap materials, $\text{Hg}_{x-1}\text{Cd}_x\text{Te}$ and, in particular, $\text{Hg}_{0.7}\text{Cd}_{0.3}\text{Te}$ have been the most widely investigated. $\text{Hg}_{0.7}\text{Cd}_{0.3}\text{Te}$ APDs have been demonstrated with highly desirable and previously unachievable avalanche gain and noise characteristics [5]. Measurements indicate that electron impact ionization dominates the avalanche multiplication in $\text{Hg}_{0.7}\text{Cd}_{0.3}\text{Te}$ APDs, resulting in theoretically minimal excess noise and leading to the devices being referred to as electron APDs (e-APDs). However, $\text{Hg}_{1-x}\text{Cd}_x\text{Te}$ remains inaccessible to many and challenging to grow and process. Hence, it would be desirable if similar performance could be achieved using a more widely available III–V material. Recently published work has shown that InAs has the potential to meet this desire, exhibiting similar electron-dominated avalanche multiplication and commensurate low excess noise [6], [7]. It is noted that the use of InAs in APDs is not without its own issues. The maximum substrate diameter available at present is 3 in; InAs has an accepted predisposition for surface leakage currents and is one of the least well developed of the binary III–V alloys. However, with further development addressing the fabrication and surface passivation in particular, they may mature into a useful technology.

Predicting or explaining the impact ionization characteristics of a material from its band structure is difficult, as, usually, the energies required for impact ionization to take place lie above the first conduction band. In InAs and $\text{Hg}_{0.7}\text{Cd}_{0.3}\text{Te}$, however, a relatively simple case can be made for preferential electron impact ionization [5], [6], [8]. In these materials, electrons can be heated by an electric field to energies well in excess of the bandgap energy, while still confined to the Γ valley of the first conduction band. Due to the low polar optical phonon-dominated scattering experienced by the electrons in the Γ valley, they should be able to rapidly attain energies well in excess of the bandgap and, hence, have the potential to impact ionization, as long as suitable states are available for the carriers. In contrast, the relatively flat heavy hole band limits the

Manuscript received March 31, 2010; revised June 4, 2010; accepted June 23, 2010. Date of publication August 9, 2010; date of current version September 22, 2010. This work was supported by the Electro Magnetic Remote Sensing Defence Technology Centre Patent GB0723858.7. The review of this paper was arranged by Editor L. Lunardi.

The authors are with the Department of Electronic and Electrical Engineering, The University of Sheffield, S1 3JD Sheffield, U.K. (e-mail: andy.marshall@sheffield.ac.uk; j.p.david@sheffield.ac.uk; c.h.tan@sheffield.ac.uk).

Digital Object Identifier 10.1109/TED.2010.2058330

TABLE I
COMPARISON OF THE SATELLITE VALLEY SEPARATION
ENERGIES IN SELECTED MATERIALS

	GaAs [9] (eV)	InP [9] (eV)	InAs (eV)			Hg _{0.7} Cd _{0.3} Te (eV)
			[8]	[9]	[10]	
E_g^Γ	1.42	1.35	0.32	0.35	0.37	0.29 [11]
$\Delta E_g^{\Gamma-X}$	0.48	0.92	1.75	1.02	1.91	3.18 [12]
	$0.33E_g$	$0.68E_g$	$5.5E_g$	$2.9E_g$	$5.2E_g$	$11E_g$
$\Delta E_g^{\Gamma-L}$	0.28	0.59	1.10	0.72	1.16	1.97 [12]
	$0.20E_g$	$0.44E_g$	$3.4E_g$	$2.0E_g$	$3.1E_g$	$6.8E_g$
Δ_{so}	0.34	0.11	-	0.39	0.43	0.88 [12]
	$0.24E_g$	$0.08E_g$	-	$1.1E_g$	$1.2E_g$	$3.1E_g$

rate at which holes heat up. Hence, it can be hypothesized that electron ionization will occur more readily than hole ionization in InAs and Hg_{0.7}Cd_{0.3}Te, particularly under low electric fields. Table I shows the published X and L valley separation energies for a number of materials with respect to their Γ valley minimum. The full band diagrams are given in [10] for InAs, GaAs, and InP and in [12] for Hg_{0.7}Cd_{0.3}Te.

In InAs at 77 K, the spin-orbit split-off energy is approximately equal to the bandgap energy. This has led to an opposing hypothesis of preferential hole impact ionization, through so-called resonant impact ionization, initiated by holes with near-zero momentum. This was the explanation offered by Mikhailova *et al.* [13] for their reported finding that β was much greater than α in InAs. However, using a Monte Carlo model, Brennan and Mansour [14] were unable to replicate the α published by Mikhailova *et al.*, instead reporting it to be much higher and exhibiting notably weaker electric field dependence. The α modeled by Brennan and Mansour was broadly supported by Marshall *et al.* [6] who found experimentally that α was much greater than β in InAs at room temperature. It is noted, however, that the conditions to support resonant hole ionization do not exist in InAs at room temperature. Other reports of avalanche multiplication dominated by resonant hole impact ionization have been made following investigations of Al_xGa_{1-x}Sb, where $x \sim 0.05$, although not all measurements have identified the same ionization coefficient ratio, and some inconsistency remains [15].

In this paper, the initial material characterization reported in [6] and [7] is extended with a systematic study of avalanche multiplication in a range of InAs p-i-n and n-i-p diodes. Through the characterization of diodes with intrinsic widths between 0.8 and 3.5- μ m and the use of different primary photogenerated carrier injection profiles, some of the key characteristics of InAs e-APDs are derived for the first time. Furthermore, the first room temperature local ionization coefficient for electrons in InAs is calculated and used to model avalanche gain. Although this paper is primarily concerned with the exploitation of impact ionization in InAs e-APDs, an accurate ionization coefficient for InAs is also beneficial to those developing transistors that use InAs, in which impact ionization has a deleterious effect [16]. In such cases, an ionization coefficient could be used to set an upper limit on the acceptable electric field in order to avoid impact ionization.

TABLE II
STRUCTURES OF THE DIODES CHARACTERIZED AS DETERMINED BY
SIMS AND $C-V$ MEASUREMENTS (BRACKETED VALUES IN ITALICS)

	Intrinsic region		p-type cladding		n-type cladding	
	width (μ m)	doping ($\times 10^{15}$ cm ⁻³)	width (μ m)	doping ($\times 10^{18}$ cm ⁻³)	width (μ m)	doping ($\times 10^{18}$ cm ⁻³)
P1	0.8 (0.9)	~ 1 (1)	2.3	5	1.9	2
P2	1.9 (1.9)	- (2)	2.3	5	1.9	5
P3	3.5 (3.5)	~ 0.2 (0.2)	1.0	6	1.9	2
N1	1.1 (1.15)	- (0.9)	1.1	0.9	0.6	8
N2	1.8 (1.8)	~ 2 (1)	2.2	5	2.0	3
N3	2.1 (2.2)	~ 1 (1)	1.4	2	0.6	4

II. DEVICE GROWTH AND FABRICATION

Homojunction InAs p-i-n and n-i-p diodes were grown by molecular beam epitaxy on InAs substrates. The growth conditions given in [17] were developed through trial growths, with the primary aim being to reduce the defect density and reverse leakage current. Minimizing the unintentional background doping concentration in the intrinsic layer was also a growth target, so that the diodes could become fully depleted at low reverse biases, and the electric field profile could be approximated to that of an ideal p-i-n type diode. All p-i-n diodes included an AlAs_{0.16}Sb_{0.84} minority electron diffusion blocking layer under the p-type InAs contact layer [17]. Circular mesa diodes of 25, 50, 100, and 200- μ m radii were then fabricated by wet etching.

The grown doping concentrations and layer thickness, as shown in Table II, were primarily confirmed by secondary ion mass spectroscopy (SIMS). Capacitance-voltage ($C-V$) measurements at 77 K were also used to confirm the approximate intrinsic width and the background doping concentration. $C-V$ measurements at room temperature were found to be inaccurate due to the relatively high reverse leakage current present. The unintentional background doping by Be and Si was found to be approximately 1×10^{15} atoms/cm³ or less, which enabled even the thickest intrinsic layers to become fully depleted by 2-V reverse bias. From forward-biased current-voltage measurements, all diodes were found to have ideality factors between 1.05 and 1.4, while diodes with radii of 100- μ m or greater had series resistances less than 20 Ω . Bulk-dominated leakage current was achieved in the best diodes.

III. RESULTS

Phase-sensitive detection was used for all photomultiplication measurements to differentiate accurately between the photocurrent and the leakage current. All measurements were performed at 293 ± 1 K. The primary photocurrent generation and other considerations were as described in [6], such that the multiplication initiated by pure electron injection (M_e) was measured on p-i-n diodes, and approximately, the multiplication due to pure hole injection (M_h) was measured on n-i-p diodes, as shown in Figs. 1 and 2, respectively. The

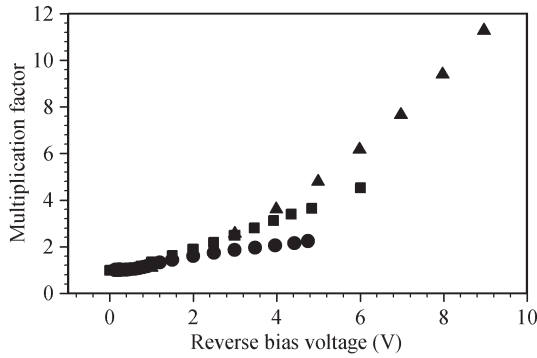


Fig. 1. M_e measured on p-i-n diodes P1 (●), P2 (■), and P3 (▲).

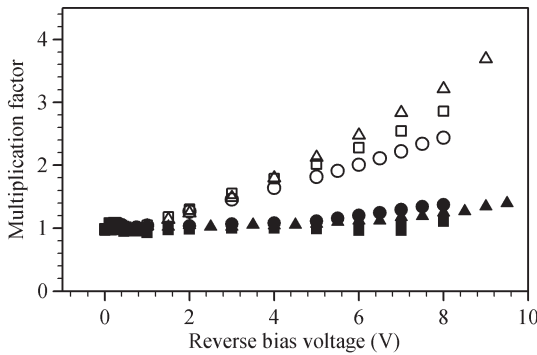


Fig. 2. Approximately (solid symbols) M_h and (open symbols) M_{mixed} , measured on n-i-p diodes N1 (●), N2 (■), and N3 (▲).

measurement results from n-i-p diodes are considered to be approaching the true M_h , overestimating the multiplication to a degree. By using a laser with a wavelength of $3.39\text{-}\mu\text{m}$, it was possible to photogenerate primary carriers in all three regions of the n-i-p diodes. The multiplication M_{mixed} of this mixed primary photocurrent is also shown in Fig. 2. All results reported are from $200\text{-}\mu\text{m}$ radii diodes. Higher multiplication could be measured on smaller diodes, as shown in Fig. 6.

The diodes' excess noise characteristics were established by measuring the photocurrent noise power using a custom phase-sensitive setup [18]. The specific experimental considerations for this measurement on InAs diodes are described in [7]. The measurements were performed at an uncontrolled room temperature of approximately 295 K. Due to the magnitude of the leakage current in the diodes, it was not possible to accurately measure the photocurrent noise power on large diodes. Indeed, it was not possible to reliably determine the excess noise factor on N1 and P1 diodes at all. It was possible to characterize N2, N3, P2, and P3 diodes with $25\text{-}\mu\text{m}$ and $50\text{-}\mu\text{m}$ radii and P3 diodes with $100\text{-}\mu\text{m}$ radii. Restricting the characterization to smaller diodes resulted in some discernable contamination being introduced to the targeted pure electron or hole injection primary photocurrents, as described in [7], due to the limitations of the optical setup used. It was found that n-i-p diodes were particularly susceptible to contamination of the primary hole photocurrent, while the contamination to the primary electron photocurrent in p-i-n diodes was much less significant, although still evident in the excess noise results. Hence, the excess noise measured on the largest area p-i-n diodes is considered to be approaching or equal to the excess noise for pure electron

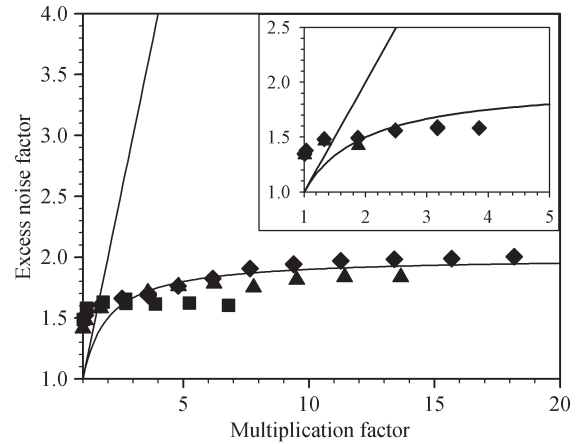


Fig. 3. Excess noise measured on P3 and P2 (inset) diodes with radii of $25\text{-}\mu\text{m}$ (◆), $50\text{-}\mu\text{m}$ (▲), and $100\text{-}\mu\text{m}$ (■). Reference lines from the local model [2] for $k = 0$ and 1 .

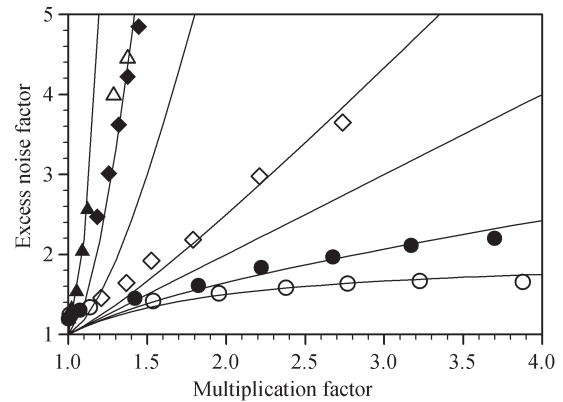


Fig. 4. Excess noise characteristics measured with predominately hole primary photocurrent on (open symbols) N2 and (solid symbols) N3 diodes with radii of $25\text{-}\mu\text{m}$ (◆) and $50\text{-}\mu\text{m}$ (▲), together with those measured with intentional mixed primary photocurrents (●) on diodes with $25\text{-}\mu\text{m}$ radii. Reference lines from the local model [2] for $k = 0, 0.3, 1, 2, 10, 30,$ and 120 .

initiated multiplication F_e , while the excess noise expected for truly pure hole initiated multiplication F_h should be notably higher than that measured on the n-i-p diodes with $50\text{-}\mu\text{m}$ radii.

IV. DISCUSSION

A. Photomultiplication Characteristics

From Figs. 1–4, it can be seen that all six InAs diodes characterized support the finding that $\alpha \gg \beta$ in InAs at room temperature. Furthermore, it is concluded that, at room temperature, it is reasonable to describe InAs APDs as e-APDs, since hole impact ionization is negligible. Interestingly, the multiplication measured at a given bias is found to be greater when the depletion width is larger, and, hence, the electric field is lower. This trend is counter to that observed in all established APDs, where the gain is always higher for a given bias if the depletion width is narrower. It is considered that the unique dependence in InAs diodes results from a combination of the very large α/β ratio and α having weak electric field dependence. Indeed, modeling has shown that atypical trends

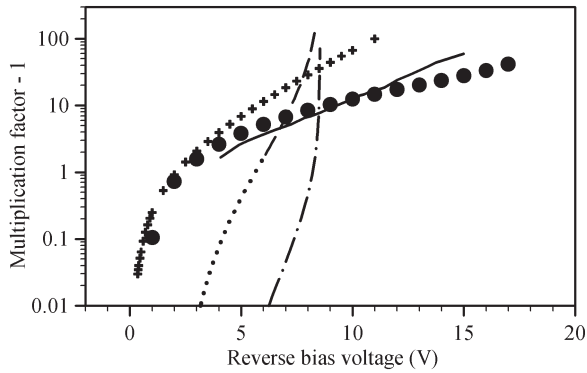


Fig. 5. Photomultiplication characteristics measured and modeled for the P3 diode structure, including the M_e measured in this paper (●), the M_e modeled with the α from Brennan and Mansour [14] setting $\beta = 0$ (crossed line), and both the M_e (dot-dashed line) and M_h (dashed line, dotted only where β is extrapolated) using α (extrapolated) and β from Mikhailova *et al.* [13]. Also shown is the M_{mixed} modeled by Satyanadh *et al.* [21] for a p-i-n diode with a 4- μm -wide intrinsic width (solid black line).

are also expected in HgCdTe e-APDs [19], [20], although these differ slightly from the trend identified here for InAs e-APDs.

Arguably, the work most comparable to this new experimental investigation is that of Satyanadh *et al.* [21], who modeled avalanche multiplication in InAs at room temperature using a Monte Carlo model. Unfortunately, drawing comparisons with their results is difficult for two reasons. First, they selected a primary carrier injection profile that cannot be replicated on practical devices, injecting electron-hole pairs uniformly across the intrinsic region of p-i-n diodes. Second, they make no mention of whether they find $\alpha > \beta$ or $\beta > \alpha$, nor can this be inferred due to the uniform mixed primary carrier injection. Their modeled avalanche multiplication for a p-i-n diode with a 4- μm intrinsic region is shown in Fig. 5. The logarithm of multiplication minus one scale is chosen to show the low gain characteristics clearly. From the linear rise on this scale, it can, at least, be concluded that the multiplication modeled was dominated by impact ionization of just one carrier type, as discussed in more detail later. The magnitude of the multiplication is similar to the M_e measured on the comparable P3 diodes, although the primary photocurrent differs. Given that impact ionization of only one carrier type appears to have dominated in the model, the multiplication expected for injection of only the most readily impact ionizing carrier type would be approaching double that reported. Despite this difference in the magnitude of the multiplication, the overall agreement with the new measured characteristics is good, particularly considering that the model was established without fitting to experimental data.

If the ionization coefficients given by Mikhailova *et al.* [13] are used to model M_e and M_h for an ideal p-i-n diode approximation of P3, they do not match the measured M_e . The most significant discrepancy is that the modeled M_e and M_h , shown in Fig. 5, break down at ~ 8 V, while stable linear mode gain is measured in P3 diodes to double this voltage. The reason for this fundamental contradiction is unclear. In contrast, if the α modeled by Brennan *et al.* [14] is parameterized and used to model M_e for P3 diodes, taking β to be zero, the result has more in common with the measured M_e .

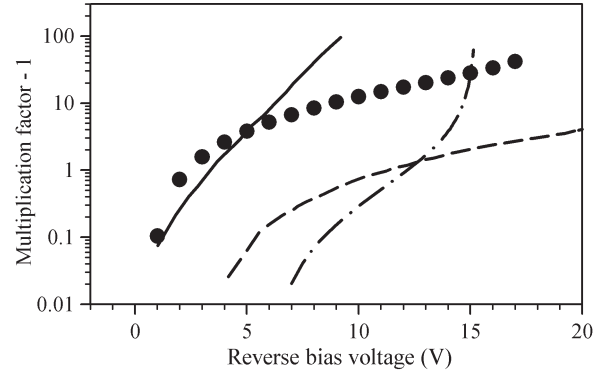


Fig. 6. Comparison between the M_e measured in this paper on P3 diodes (●) and multiplication characteristics measured on other materials, including HgCdTe, with cutoff wavelengths of 4.2- μm (solid back line) and 2.2- μm (dashed black line) [5] and InAlAs (dot-dashed line) [22].

The avalanche multiplication resulting from the impact ionization of only one carrier type, as in an e-APD, is characteristically different from that resulting when both carrier types undergo impact ionization. Fig. 6 compares the multiplication measured on a P3 InAs diode with that measured on InAlAs [22] and HgCdTe APDs [5]. The InAlAs APD's multiplication characteristic is typical of APDs, where both carrier types undergo impact ionization; gain is negligible at low bias voltages before rising rapidly to a sharp breakdown. Although this multiplication characteristic would shift along the voltage scale where the depletion width changes, its characteristic shape would remain. In contrast, when only one carrier type undergoes impact ionization, the absence of a feedback mechanism leads to an exponentially rising gain without an avalanche breakdown. The multiplication characteristics from InAs and HgCdTe diodes match this e-APD model, rising linearly on the logarithmic scale, after an initial turn-on. It is interesting to consider the bias dependence of the multiplication characteristics shown in Fig. 6, in relation to the concomitant requirements for the APD's biasing circuit. Typically, APDs need to be accurately and stably biased to maintain the desired operational gain. However, the absence of feedback impact ionization in e-APDs makes their gain less sensitive to fluctuations in bias voltage, which could provide a system-level advantage.

From Fig. 6, it is evident that avalanche multiplication in InAs APDs starts at a very low voltage. Indeed, electron avalanche multiplication in InAs p-i-n diodes was found to turn on by 0.4–0.5 V in all cases. For this to be possible, the impact ionization threshold energy must be low. C - V measurements indicate that the built-in potential in these diodes is in the order of 0.05 V, resulting in a maximum energy gain for electrons injected from the p-type cladding of ~ 0.50 eV, under an external bias of 0.45 V and assuming a ballistic transport model. However, the electron ionization threshold energy must be ≥ 0.36 eV, the bandgap energy. Hence, even ballistic electrons can only gain a maximum of 0.14 eV more than the minimum ionization threshold energy while traveling up to 2- μm . For a significant fraction of the electrons transiting the depletion region to lose less than 0.14 eV and, hence, for impact ionization to be possible with an applied bias of just 0.45 V, energy loss through scattering must be very low.

Carriers moving in the wider bandgap materials currently used in APDs experience much higher scattering rates, which means that higher electric fields are required to initiate avalanche multiplication. Hence, the presence of avalanche multiplication at low electric fields is a further clear distinction between the emerging narrow bandgap e-APDs and established wider bandgap APDs.

It is clear that impact ionization of electrons from within the Γ valley does occur in InAs and aided by the low scattering rates it does so even at very low electric fields. Although it would be simple to consider that all impact ionization of electrons was initiated from within the Γ valley, this appears unlikely. The ionization threshold appears to be soft and the ionization rate limited at the lower energies in excess of it. It is considered inevitable that some electrons will leave the confines of the Γ valley in the practical devices characterized. Hence, a multivalley Monte Carlo model will be needed to faithfully model the nonlocal nature of impact ionization in InAs; however, it is likely that only the first conduction band needs to be considered.

Due to β being approximately zero, it is noted that the impulse response duration for InAs e-APDs should be no greater than the sum of one transit time for electrons and one transit time for holes. This should make operation at high bit rates possible, even with wide depletion regions such as those characterized in this paper. Based on the saturated electron drift velocity modeled by Satyanadh *et al.* [21] and the saturated hole drift velocity of $\text{In}_{0.53}\text{Ga}_{0.47}\text{As}$, the maximum bit rate achievable without intersymbol interference can be estimated. It is concluded that an InAs p-i-n diode with a $2.5\text{-}\mu\text{m}$ -wide intrinsic region could support bit rates up to ~ 20 Gb/s. Furthermore, with $\beta \sim 0$, the impulse response duration should be independent of gain. The resulting absence of a classical gain-bandwidth product limit should make it possible to exploit much higher gains in thicker devices at bit rates only limited by the same double transit time constraint.

B. Excess Noise Characteristics

The multiplication dependence of an e-APDs excess noise factor is also fundamentally different from that of conventional APDs. The excess noise characteristic of an InAlAs APD shown in Fig. 7 is representative of the current state of the art telecommunication APDs. In such APDs, the excess noise factor continues to rise as multiplication increases, as is expected whenever $k > 0$. Besides the new results for InAs APDs, the only published excess noise results less than or equal to the local model's prediction for $k = 0$ come from HgCdTe. One such result from an APD with a cutoff wavelength of $2.2\text{-}\mu\text{m}$ is shown in Fig. 7. It is noted that the excess noise characteristic modeled by Satyanadh *et al.* for InAs APDs lies above the prediction for $k = 0$. However, for their mixed injection case, $F > F_e$ would be expected; hence, the excess noise modeled is actually very low given the mixed primary photocurrent and broadly supportive of the new experimental results.

To explain excess noise factors tending toward values below 2, such as those measured on InAs p-i-n diodes under the purest electron injection, it is necessary to consider the influence of

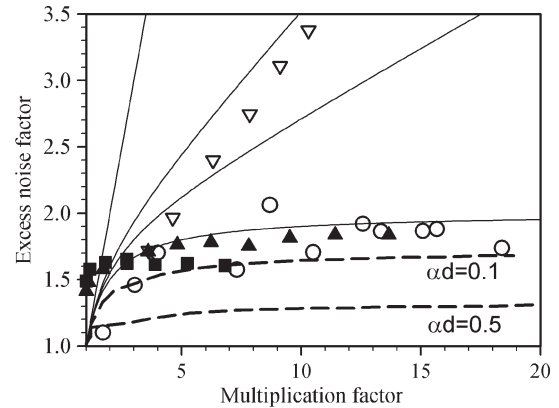


Fig. 7. Comparison between the excess noise approaching F_e measured on P3 diodes with radii of $50\text{-}\mu\text{m}$ (\blacktriangle) and $100\text{-}\mu\text{m}$ (\blacksquare) and excess noise characteristics measured on InAlAs (∇) [20] and HgCdTe (\circ) [5] diodes. Also shown are the excess noise characteristics modeled by Saleh *et al.* [24] for fixed ratios of αd (dashed black lines) and reference lines from the local model [2] for $k = 0, 0.1, 0.2, \text{ and } 1$.

ionization deadspace neglected by the local model. Deadspace is described by various authors as either the distance travelled by a carrier while it attains the ionization threshold energy or the distance travelled by a carrier while its energy rises into equilibrium with the electric field. Both descriptions attempt to address the reality that a carrier's ionization probability does not become a nonzero function, described by its nonlocal ionization coefficient, until it has travelled some distance. It is simplest to consider that it travels this distance with an ionization probability of zero, leading to the first description. However, more accurately, its ionization probability is only zero for part of the distance, before rising over the remainder of the distance, to reach that described by the nonlocal ionization coefficient. The effect of this deadspace is to increase the degree of determinism in the spatial distribution of impact ionization events, which, in turn, reduces the fluctuations in the multiplication experienced by individual carriers and, hence, the noise. In the limiting case where carriers traverse zero ionization probability deadspaces between delta function ionization probability functions, the increased order reduces the excess noise factor to a value of unity. The nonlocal nature of impact ionization is usually only found to become significant when an APD's multiplication region width is in the order of hundreds of nanometers or less [23]. However, there is no theoretical reason why deadspace cannot be significant in APDs with thicker multiplication regions.

The parameters αd or βd give a measure of the proportion of the respective overall ionization path lengths α^{-1} and β^{-1} occupied by the deadspace. The value of these parameters can range between zero and unity; the higher their value, the more deterministic the ionization path lengths of the individual carriers. Saleh *et al.* [24] modeled the excess noise characteristics for two constant values of αd , when $\beta = 0$, as shown in Fig. 7. This shows that even when $\alpha d = 0.1$, the increased determinism suppresses the excess noise significantly. In reality, a constant value of αd is not expected since α and d have different dependencies on electric field. These dependencies will lead to αd increasing with increasing electric field and increasing

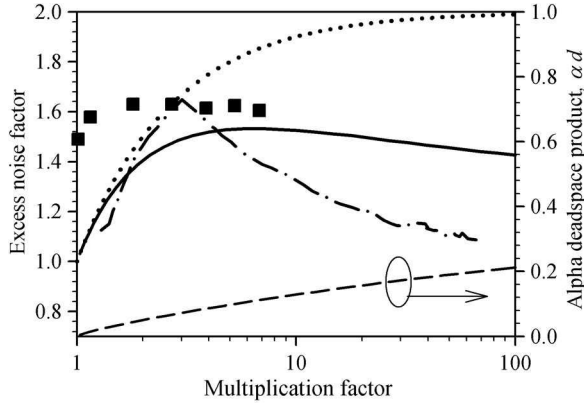


Fig. 8. Comparison of e-APD-type excess noise characteristics, including those measured on a P3 diode with a 100- μm radius (\blacksquare), modeled by Ma *et al.* [25] for HgCdTe diodes (dot-dash line) and modeled by the local model [2] for $k = 0$ (dotted line). Also shown are the excess noise factor (solid line) and αd (dashed line) modeled for an arbitrary $k = 0$ case.

multiplication factors. As shown later, α is higher in InAs at low electric fields than in most materials characterized. This contributes to αd being significant in InAs even at low electric fields, as present in P3 diodes in particular. Indeed, if the new α for InAs given later is considered, in order to obtain $\alpha d = 0.1$ at $M \sim 7$ as seen in Fig. 7 for a P3 diode, a deadspace of ~ 170 nm or ≤ 0.35 eV is needed. Given that the true F_e is considered to be less than or equal to the result shown in Fig. 7 for a 100- μm radius diode, this calculation should be considered to indicate the minimum ionization threshold energy. If there is a perfectly pure injection to yield a lower F , matching a higher αd , the calculated threshold energy would also be higher. However, 0.35 eV is approximately equal to the bandgap energy for InAs and plausible considering that the electron ionization threshold energy is expected to approach the bandgap energy when $m_e \ll m_h$, as is the case for InAs. Indeed, this magnitude of threshold energy is also supported by the onset of measurable multiplication at low reverse biases, as discussed earlier.

It is observed that the excess noise characteristic shown in Fig. 7 for a 100- μm radius P3 diode rises to a peak before decreasing slightly with increasing multiplication. This is considered to be caused by αd increasing as the bias voltage and the electric field increase. Modeling of the excess noise in HgCdTe APDs by Ma *et al.* [25] showed a more pronounced peaking, as shown in Fig. 8. Also shown in Fig. 8 is the excess noise characteristic modeled using the published nonlocal α and threshold energy for GaAs [26], with β set to zero. This arbitrary case was modeled using a random path length model, from which the commensurate values of αd could also be calculated. As can be seen from Fig. 8, for this modeled case, αd rises as the multiplication and the electric field increase, while, again, the excess noise factor peaks and then falls.

C. Electron Ionization Coefficient

The new measurements of multiplication and excess noise on a range of InAs diodes have confirmed that $\beta \sim 0$ at room temperature; hence, a simple local electron ionization coefficient

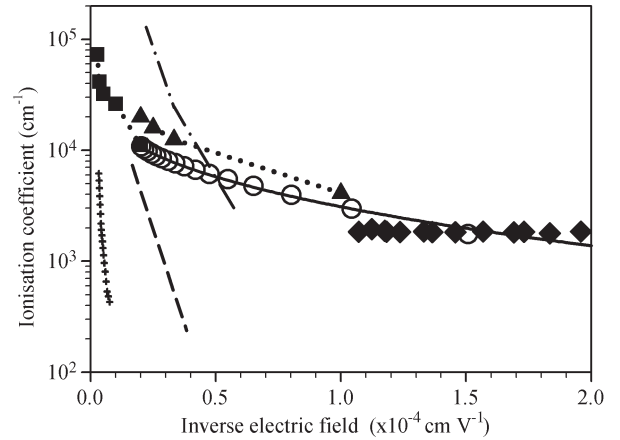


Fig. 9. Comparison of modeled and experimentally derived ionization coefficients, including α for InAs from this paper as calculated (\circ) and as parameterized (solid line), α (dashed line) and β (dot-dashed line) for InAs from Mikhailova *et al.* [13], α for InAs from Bude and Hess [8] (\blacksquare), α for InAs from Brennan and Mansour [14] (\blacktriangle), α for $\text{In}_{0.53}\text{Ga}_{0.47}\text{As}$ from Ng *et al.* [27] (crossed line), and α for InSb from Baertsch [28] (\blacklozenge).

can be calculated from M_e alone. Despite having the widest intrinsic region, in practice, P3 diodes yielded M_e results up to similar internal electric fields to the other p-i-n samples. Hence, the M_e measured on P3 diodes alone is used to calculate α , while the M_e characteristics measured on P1 and P2 diodes are used to cross check its validity. The calculation of α is simplified by two approximations. First, the electric field is taken to be constant. The electric field ξ is calculated from ideal p-i-n structure approximations, where the intrinsic width W is taken to be equal to the total depletion width modeled at each given bias voltage using the doping profile measured by SIMS. The ideal p-i-n approximation is considered reasonable for P3 diodes due to their very low background doping concentration, confirmed by C - V measurements. Second, β is taken to be zero such that α can be calculated from

$$\alpha(\xi) = \frac{1}{W} \ln(M_e(V)). \quad (1)$$

The α calculated in this way is shown in Fig. 9. By comparison, the α calculated by Mikhailova *et al.* [13] shows much stronger dependence on the electric field, falling much more rapidly with reducing electric field. Brennan and Mansour [14] calculated α for a number of different scattering conditions. Even their lowest α , shown in Fig. 9, is higher than the new calculated α ; however, the electric field dependence is very similar. Bude and Hess [8] calculated α for InAs in a higher electric field range than it was possible to exercise in the practical diodes. However, their α does align with the magnitude of α calculated here at the highest electric fields. $\text{In}_{0.53}\text{Ga}_{0.47}\text{As}$ has the lowest bandgap energy among the more established III-V materials for which ionization coefficients have been published. Amongst such materials, it has an unusually high α at lower electric fields [27]; however, compared with the new α for InAs, it is lower and much more strongly dependent on the electric field. Baertsch [28] calculated an experimentally derived α for InSb at 77 K. This α exhibits almost no electric field dependence, but a similar magnitude to the new α for InAs.

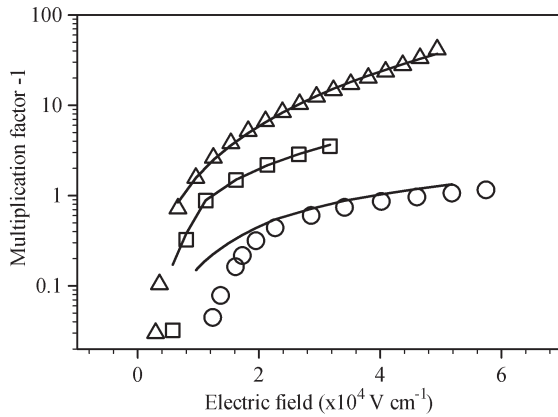


Fig. 10. Comparison between the multiplication measured on P1 (\circ), P2 (\square), and P3 (\triangle) diodes and that modeled (lines) using the new α and $\beta = 0$.

The new α has been parameterized, for electric fields between 6 and 50 kV/cm, as

$$\alpha = 4.62 \times 10^4 \exp \left[- \left(\frac{1.39 \times 10^5}{|\xi|} \right)^{0.378} \right] \text{ cm}^{-1}. \quad (2)$$

The capability of the new ionization coefficient to model avalanche multiplication in InAs APDs is confirmed by the comparison shown in Fig. 10. The new coefficient proves to be both self-consistent and capable of modeling the multiplication measured in P1 and P2 diodes. The fit to the results for P1 diodes is not as good as the fit to the results for P2 diodes; however, this is thought to be a result of the ideal p-i-n structure approximation used being less valid for P1 diodes.

As a result of α being much greater at low electric fields in InAs than in wider bandgap III-V materials, all InAs APDs realized to date operate in the electric field range for which impact ionization is essentially nonexistent in wider bandgap materials. Hence, it is concluded that the relatively enhanced magnitude of α is responsible for the desirable $k \sim 0$ characteristic in these InAs APDs, rather than an atypically low magnitude of β . If measurements were possible at sufficiently higher electric fields, it is considered probable that β would be broadly similar to that measured in other materials such as $\text{In}_{0.53}\text{Ga}_{0.47}\text{As}$. However, this is expected to prove impossible in practice due to the onset of tunneling.

V. CONCLUSION

The results of an extensive study into the characteristics of InAs APDs have been presented. It has been shown that α is significant, while $\beta \sim 0$ in the electric field range exercised, leading to e-APD-type characteristics. An electron ionization coefficient has been calculated and verified. This coefficient will be of use to those designing InAs-based APDs and transistors. The multiplication and excess noise characteristics of InAs APDs and e-APDs in general have been considered. It has been shown that not only does impact ionization of electrons occur within the Γ valley but, aided by the low scattering rates, it also does so from very low electric fields. Furthermore, nonlocal effects can be significant even in diodes

with thick depletion regions. A unique dependence of M_e on depletion width and bias voltage in InAs e-APDs has also been identified. Now, since these scientifically and practically interesting characteristics have been demonstrated in a simple III-V binary alloy, there is a potential for further widespread study or exploitation. InAs e-APDs are likely to be of interest in infrared focal plane array imaging applications, where their low operating voltage is advantageous. They may also find application in optical communications, aided by an absence of a gain bandwidth product, or single-photon detection.

REFERENCES

- [1] J. P. R. David and C. H. Tan, "Material considerations for avalanche photodiodes," *IEEE J. Sel. Topics Quantum Electron.*, vol. 14, no. 4, pp. 998–1009, Jul. 2008.
- [2] R. J. McIntyre, "Multiplication noise in uniform avalanche diodes," *IEEE Trans. Electron Devices*, vol. ED-13, no. 1, pp. 164–168, Jan. 1966.
- [3] R. B. Emmons, "Avalanche-photodiode frequency response," *J. Appl. Phys.*, vol. 38, no. 9, pp. 3705–3714, Aug. 1967.
- [4] J. C. Campbell, "Recent advances in avalanche photodiodes," *IEEE J. Sel. Topics Quantum Electron.*, vol. 10, no. 4, pp. 777–787, Jul. 2004.
- [5] J. Beck, C. Wan, M. Kinch, J. Robinson, P. Mitra, R. Scritchfield, F. Ma, and J. Campbell, "The HgCdTe electron avalanche photodiode," *J. Electron. Mater.*, vol. 35, no. 6, pp. 1166–1173, 2006.
- [6] A. R. J. Marshall, C. H. Tan, M. J. Steer, and J. P. R. David, "Electron dominated impact ionization and avalanche gain in InAs photodiodes," *Appl. Phys. Lett.*, vol. 93, no. 11, p. 111107, Sep. 2008.
- [7] A. R. J. Marshall, C. H. Tan, M. J. Steer, and J. P. R. David, "Extremely low excess noise in InAs electron avalanche photodiodes," *IEEE Photon. Technol. Lett.*, vol. 21, no. 13, pp. 866–868, Jul. 2009.
- [8] J. Bude and K. Hess, "Thresholds of impact ionization in semiconductors," *J. Appl. Phys.*, vol. 72, no. 8, pp. 3554–3561, Oct. 1992.
- [9] I. Vurgaftman, J. R. Meyer, and L. R. Ram-Mohan, "Band parameters for III-V compound semiconductors and their alloys," *J. Appl. Phys.*, vol. 89, no. 11, pp. 5815–5875, Jun. 2001.
- [10] J. R. Chelikowsky and M. L. Cohen, "Nonlocal pseudopotential calculations for the electronic structure of eleven diamond zinc-blende semiconductors," *Phys. Rev. B, Condens. Matter*, vol. 14, no. 2, pp. 556–582, Jul. 1976.
- [11] Y. Marfaing, "Optoelectronics with II-VI and IV-VI compounds," *Mater. Sci. Eng. B*, vol. 9, no. 1–3, pp. 169–177, Jul. 1991.
- [12] R. D. Graft, "Localized orbital description of the electronic structure of $\text{Hg}_{(1-x)}\text{Cd}_x\text{Te}$ pseudobinary alloys," *J. Vac. Sci. Technol.*, vol. 21, no. 1, pp. 146–148, May 1982.
- [13] M. P. Mikhailova, M. M. Smirnova, and S. V. Slobodchikov, "Carrier multiplication in InAs and InGaAs p-n junctions and their ionization coefficients," *Sov. Phys. Semicond.*, vol. 10, no. 5, pp. 509–513, May 1976.
- [14] K. F. Brennan and N. S. Mansour, "Monte Carlo calculation of electron impact ionization in bulk InAs and HgCdTe," *J. Appl. Phys.*, vol. 69, no. 11, pp. 7844–7847, Jun. 1991.
- [15] H. Luquet, M. Perotin, L. Gouskov, C. Linares, H. Archidi, M. Lahbabi, M. Karim, and B. Mbow, "Ionization coefficients in $\text{Ga}_{0.96}\text{Al}_{0.04}\text{Sb}$," *J. Appl. Phys.*, vol. 68, no. 8, pp. 3861–3864, Oct. 1990.
- [16] B. Brar and H. Kroemer, "Influence of impact ionization on the drain conductance in InAs-AlSb quantum well heterostructure field-effect transistors," *IEEE Electron Device Lett.*, vol. 16, no. 12, pp. 548–550, Dec. 1995.
- [17] A. R. J. Marshall, C. H. Tan, J. P. R. David, J. S. Ng, and M. Hopkinson, "Fabrication of InAs photodiodes with reduced surface leakage current," in *Proc. SPIE Opt. Mater. Defence Syst. Technol.*, 2007, vol. 6740, p. 67400H.
- [18] K. S. Lau, C. H. Tan, B. K. Ng, K. F. Li, R. C. Tozer, J. P. R. David, and G. J. Rees, "Excess noise measurement in avalanche photodiodes using a transimpedance amplifier front-end," *Meas. Sci. Technol.*, vol. 17, no. 7, pp. 1941–1946, Jun. 2006.
- [19] S. Derelle, S. Bernhardt, R. Haidar, J. Deschamps, J. Primot, J. Rothman, S. Rommeluere, and N. Guerineau, "Experimental performances and Monte Carlo modelling of LWIR HgCdTe avalanche photodiodes," in *Proc. SPIE Opt. Sens.*, May 2009, vol. 7356, p. 735627.
- [20] M. Kinch, "A theoretical model for the HgCdTe electron avalanche photodiode," *J. Electron. Mater.*, vol. 37, no. 9, pp. 1453–1459, Apr. 2008.

- [21] G. Satyanadh, R. P. Joshi, N. Abedin, and U. Singh, "Monte Carlo calculation of electron drift characteristics and avalanche noise in bulk InAs," *J. Appl. Phys.*, vol. 91, no. 3, pp. 1331–1338, Feb. 2002.
- [22] Y. L. Goh, A. R. J. Marshall, D. J. Massey, J. S. Ng, C. H. Tan, M. Hopkinson, J. P. R. David, S. K. Jones, C. C. Button, and S. M. Pinches, "Excess avalanche noise in $\text{In}_{0.52}\text{Al}_{0.48}\text{As}$," *IEEE J. Quantum Electron.*, vol. 43, no. 6, pp. 503–507, Jun. 2007.
- [23] S. A. Plimmer, J. P. R. David, and D. S. Ong, "The merits and limitations of local impact ionisation theory," *IEEE Trans. Electron Devices*, vol. 47, no. 5, pp. 1080–1088, May 2000.
- [24] B. E. A. Saleh, M. M. Hayat, and M. C. Teich, "Effect of dead space on the excess noise factor and time response of avalanche photodiodes," *IEEE Trans. Electron Device*, vol. 37, no. 9, pp. 1976–1984, Sep. 1990.
- [25] F. Ma, X. Li, J. Campbell, J. Beck, C.-F. Wan, and M. A. Kinch, "Monte Carlo simulations of $\text{Hg}_{0.7}\text{Cd}_{0.3}\text{Te}$ avalanche photodiodes and resonance phenomenon in the multiplication noise," *Appl. Phys. Lett.*, vol. 83, no. 4, pp. 785–787, Jul. 2003.
- [26] S. A. Plimmer, J. P. R. David, G. J. Rees, and P. N. Robson, "Ionisation coefficients in $\text{Al}_x\text{Ga}_{1-x}\text{As}$ ($x = 0 - 0.60$)," *Semicond. Sci. Technol.*, vol. 15, no. 7, pp. 692–699, Jul. 2000.
- [27] J. S. Ng, C. H. Tan, J. P. R. David, G. Hill, and G. J. Rees, "Field dependence of impact ionisation coefficients in $\text{In}_{0.53}\text{Ga}_{0.47}\text{As}$," *IEEE Trans. Electron Devices*, vol. 50, no. 4, pp. 901–905, Apr. 2003.
- [28] R. D. Baertsch, "Noise and multiplication measurements in InSb avalanche photodiodes," *J. Appl. Phys.*, vol. 38, no. 11, pp. 4267–4274, Oct. 1967.

Andrew R. J. Marshall received the M.Eng. (with honors) degree in electronic and electrical engineering in 1999 from The University of Sheffield, Sheffield, U.K., where he is currently working toward the Ph.D. degree.

In 1999, he joined the Ford Motor Company, and, in 2000, he joined Visteon, where he worked on the design and manufacturing of car instruments and displays until 2004. Since 2008, he has been a Researcher with the Department of Electronic and Electrical Engineering, The University of Sheffield. His research interests include the theory, characterization, and fabrication of high-performance photodiodes and avalanche photodiodes.

Mr. Marshall became a Chartered Engineer in 2005.

John P. R. David (SM'96) received the B.Eng. and Ph.D. degrees in electronic engineering from The University of Sheffield, Sheffield, U.K.

In 1985, he was with the Central Facility for III–V Semiconductors, Sheffield, where he was involved in the characterization activity. In 2001, he was with Marconi Optical Components (now Bookham Technologies). He is currently a Professor with the Department of Electronic and Electrical Engineering, The University of Sheffield. His current research interests include piezoelectric III–V semiconductors and impact ionization in analog and single-photon avalanche photodiodes.

Dr. David was an IEEE Lasers and Electro Optics Society Distinguished Lecturer from 2002 to 2004.

Chee Hing Tan (M'95) received the B.Eng. and Ph.D. degrees in electronic engineering from The University of Sheffield, Sheffield, U.K., in 1998 and 2002, respectively.

Since 2003, he has been with the Department of Electronic and Electrical Engineering, The University of Sheffield, where he was a Lecturer and, currently, a Senior Lecturer. He has extensive experience in characterization and modeling of high-speed low-noise avalanche photodiodes and phototransistors. His current research interests include single-photon avalanche diodes, mid-infrared photodiodes, quantum dot infrared detectors, and ultrahigh speed avalanche photodiodes and phototransistors.